Effect of Rheology on Coalescence Rates and Emulsion Stability

T. M. Dreher, J. Glass, A. J. O'Connor, and G. W. Stevens
Dept. of Chemical Engineering, The University of Melbourne, Parkville, Victoria, 3052, Australia

The effect of continuous-phase rheology on the coalescence time of single water drops at an organic/aqueous interface was investigated experimentally. For Newtonian fluids, the coalescence time increases monotonically with the continuous-phase viscosity at a fixed drop diameter and with the drop diameter at a fixed continuous-phase viscosity. Elasticity in the continuous phase caused significant increases in the coalescence times for drops of less than 1 mm diameter in the systems studied, but had no discernible effect on the coalescence of larger drops. Estimates of the interfacial shear rates were used to demonstrate that the elasticity of the continuous phase becomes significant in the coalescence process as the drop size decreases. These results indicate that emulsion stability may be increased without the use of surfactants by adding a suitable polymer to the continuous phase and control of the dispersed-phase drop size.

Introduction

The ability to control the stability of emulsions or the rate of coalescence of drops at an interface is important in many applications. For example, many foods such as salad dressings, mayonnaise, and ice creams are emulsions and the stability of these emulsions is important to their performance as foods. Emulsion liquid membrane processes used for water treatment also require stable emulsions in order to minimize mixing of the external and internal aqueous phases. By contrast, in processes such as solvent extraction, one phase is dispersed in another to enhance mass transfer and then the phases are separated; this phase separation is usually rate limiting at high throughputs, and so increased coalescence rates would be beneficial.

In many applications of emulsions, the stability of water drops in a continuous oil phase is of great interest. However, the stability of an emulsion is an extremely intricate phenomenon, and it is useful to first study the coalescence of single water drops at an oil-water interface to reduce the complexity of the investigation. Coalescence will usually occur when a drop approaches a fluid-fluid interface, where an interfacial film forms, drains to a certain thickness, and then ruptures. Film rupture is very rapid (Hartland, 1967b), and so the life of the interfacial film is largely determined by its rate of thinning. A significant distribution of coalescence times is often observed, which may be attributed to the random nature of the disturbances which cause the film to thin and break, such as vibrations, corrugations at the interface, thermal, velocity, and interfacial tensions gradients (Vrij and Overbeek, 1968; Lang and Wilkie, 1971). Dell'Aversana et al. (1996, 1997) have shown that coalescence can be prevented under special conditions involving the flow of the interfaces (such as those driven by applied thermal or shear gradients). However, such conditions cannot be imposed on emulsions in practical applications.

A variety of models exist relating drop coalescence times to the physical properties of two-fluid systems. Early models considered coalescence to be a purely hydrodynamic phenomenon: for example, Gillespie and Rideal (1956) assumed that the fluid interfaces behave as two flat plates to obtain the following expression for coalescence time

$$t = \frac{a^5 \mu_c \Delta\rho g}{4\gamma^2}\left[\frac{1}{h_c^2} - \frac{1}{h_i^2}\right] \tag{1}$$

However, dimple formation and tilting tend to result in the draining film having nonuniform thickness, so models which assume a uniform thickness have been found to underpredict the rate of film drainage (Hartland, 1967a; Murdoch and Leng, 1971). Furthermore, interfacial mobility and interfacial forces also have significant effects on the draining

Correspondence concerning this article should be addressed to G. W. Stevens.

process and need to be included in a feasible model. Hartland (1969) developed a model for the drainage of a film beneath a rigid sphere approaching a deformable fluid interface, accounting for interfacial mobility via the empirical parameter n_i, ''the number of immobile interfaces''

$$t = \frac{3n_i^2 \mu_c \{2\pi a^2 (1-\cos\alpha)\}^2}{16\pi F}\left[\frac{1}{h_c^2} - \frac{1}{h_i^2}\right] \qquad (2)$$

Some more recent models have attempted to account for other significant factors including interfacial tension gradients, fluid circulation within the phases, and surface viscosities (Barber and Hartland, 1976; Zapryanov et al., 1983; Hartland and Jeelani, 1994). However, it is generally not possible to experimentally determine all of the parameters such as the gradient of interfacial tension in the draining film, required to make accurate predictions using these models. Numerical modeling techniques have been used to predict drop shapes and film drainage rates for the limiting cases of nearly fully mobile or fully immobile interfaces (Yiantsios and Davis, 1990). However, even these limiting calculations involve significant simplifying assumptions such as negligible intermolecular forces and very small drops.

For rheologically complex fluids, coalescence phenomena have only received limited investigation and little modeling has been attempted. The squeezing flow between parallel discs may be used as a first approximation, which has been solved for Newtonian (Stefan and Sitzgber, 1874) and power-law (Scott, 1931) fluids. For the case of squeeze-film flow under constant force, many authors have predicted that viscoelastic films will thin at faster rates than a Newtonian film (Tanner, 1965; Kramer, 1974; Brindley et al., 1976), which is contradictory to experimental results (Brindley et al., 1976; Leider and Bird, 1974). The model developed by Metzner (1971) predicts that a viscoelastic fluid will squeeze out less rapidly for a given applied force in the case of fast squeezing flows. This result is especially apparent for very rapid squeezing, where the elastic fluid exhibits solid-like behavior, as the polymer molecules do not have time to realign. Although Metzner's model predicts the correct trends, Leider and Bird (1974) expressed concern over numerous deficiencies in this model, especially that it does not reduce to Scott's (1931) equation for power-law fluids when the fluid's relaxation time is zero. In contrast to the experimental and theoretical results described above, Williams and Tanner (1970) found that normal stress and elongational effects were negligible in a thin film and were, therefore, not important in viscoelastic lubrication.

Leider and Bird (1974) proposed that the inadequacy in previous models lay primarily in the choice of the rheological equation used in describing the fluid. Equation 3 was developed for a power-law fluid to describe the force on the upper plate. They were able to correctly predict trends in their experimental data, but warned that the solution is only to be regarded as an indication of the ''right'' approach, not as an analytical answer. The quantity in braces is the deviation from the solution for a power-law fluid, where λ is the relaxation time of the fluid, and c_1 and c_2 are constants, each of which may be assumed to be approximately equal to one

$$F = \left(\frac{-\dot{h}}{h^{2+1/n}}\right)^n \left(\frac{2n+1}{2n}\right)^n \frac{\pi m R^{n+3}}{n+3} \times \left\{1 + \left[\left(\frac{-\dot{h}}{h^{2+1/n}}\right)\left(\frac{2n+1}{2n}\right)\left(\frac{h_i}{2}\right)^{1/n} c_1 Rt - 1\right] \exp\left(\frac{-t}{c_2 n\lambda}\right)\right\} \qquad (3)$$

McClelland and Finlayson (1983) also developed a model for a power-law fluid including normal stress effects (Eq. 4). They were able to correctly predict the constant force results for both fast and slow squeezing, but the equation was found not to apply to constant velocity data

$$F = \frac{(-\dot{h})^n}{h^{2n+1}}\left(\frac{2n+1}{2n}\right)^n \frac{\pi m R^{n+3}}{n+3} + \frac{(-\dot{h})^{n'}}{h^{2n'}}\left(\frac{2n+1}{2n}\right)^{n'} \frac{\pi m' R^{n'+2}}{n'+2} \qquad (4)$$

The rheological parameters m, n, m', and n' are defined by $\mu = m\dot{\gamma}^{n-1}$ and $N_1 = -m'\dot{\gamma}^{n'}$. A numerical procedure was also developed for fluids having viscometric functions of arbitrary form. McClelland and Finlayson reanalyzed Brindley et al.'s (1976) model using revised rheological equations and boundary conditions, and found that it did then predict experimental results correctly. However, Phan-Thien et al. (1987) did not believe that either normal stresses alone nor elongational effects could account for observed stiffening in squeeze-film flow of viscoelastic fluids. They demonstrated, using numerical modeling, that a stress overshoot mechanism was needed to account for the observations in constant speed or constant load squeezing flows when shear flow is started suddenly. Viscoelastic effects were predicted to be significant for Weissenberg numbers ($\mathrm{Wi} = -\lambda u_i/h$) greater than 0.5 for constant speed squeezing.

These models were developed for the squeezing of a film between two flat plates. Therefore, their applicability to coalescence is limited, as they do not allow for interface deformation or mobility. They do, however, give an indication of the predicted effect of elasticity on squeeze film flow, but the fact that the models significantly overpredict the coalescence time means that interfacial mobility is an important mechanism in coalescence.

Experimental Techniques

Apparatus

The primary apparatus (Figure 1) consisted of a 355-mm long glass tube (ID = 39 mm), enclosed at the base. The tube was filled with water until the level was about 70 mm from the base, and then filled with oil to about 30 mm from the top of the tube. Filling was performed in a laminar flow hood to minimize contamination. The top of the tube was sealed with a tight fitting teflon bung and, through the center of the bung, a stainless steel syringe needle was threaded. The glass tube was placed in a tight fitting cup, which was attached to a platform that was able to be moved vertically by means of a screw. Two pairs of PN gallium arsenide infrared emitting

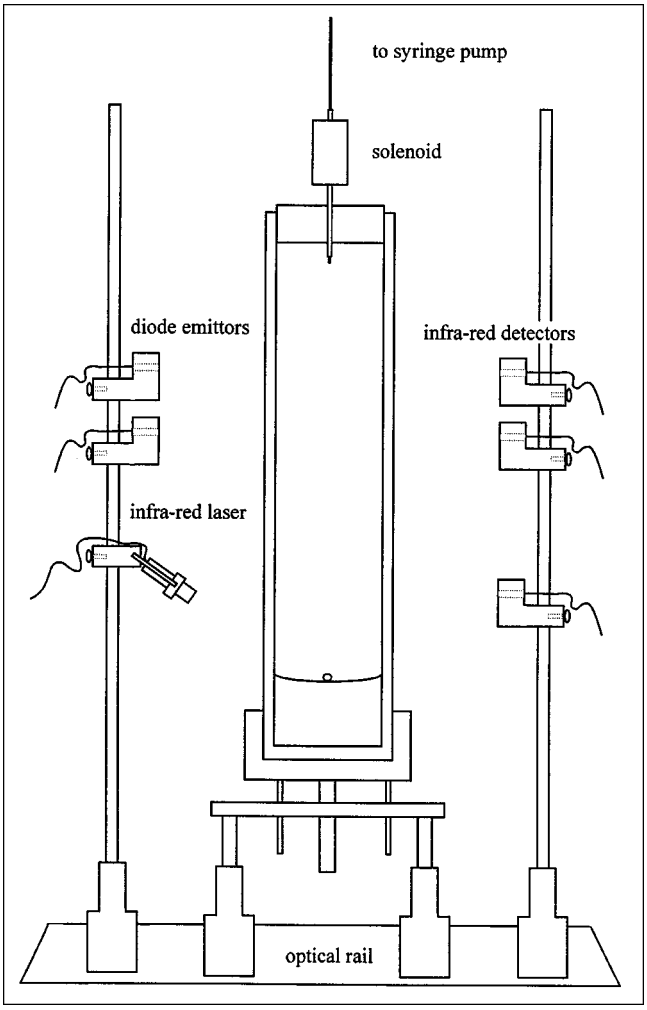

Figure 1. Coalescence apparatus.

diodes (peak emission wavelength 900 nm, NTE No. 3028) and silicon phototransistor detectors (NTE No. 3032), obtained from Stewart Electronics, were clamped to vertical rods on opposite sides of the glass tube. The first was situated about 80 mm from the syringe tip and the second was 43.7 mm lower to record the terminal velocity of the falling drops. A continuous wave infrared laser diode module (780 nm, 25 mW, Vector Technology Ltd.) and a further phototransistor detector were also clamped to the rods at a position where the laser beam bounced clearly off the oil/water interface, which was approximately 250 mm from the syringe tip. This enabled the time a drop sat at the oil/water interface to be measured, which was defined as the coalescence time. The tube and base, as well as diode rods, were all mounted on an optical rail, and experiments were conducted in a 20 ± 1°C thermostated room.

The drop delivery system consisted of a 1 mL gas tight syringe connected to a needle of 0.65 mm inside diameter and 50 mm length via a Luer lock joint. Stainless steel chromatography tubing of ID 0.25 mm and OD 0.50 mm was inserted into the needle and soldered from the outside. The needle tip was threaded through a support tube, which was then inserted through a general purpose miniature solenoid. The solenoid was connected to a multifunctional digital timer to control the time of drop release. The syringe and needle parts were obtained from SGE Scientific, and the electronics from RS Components. The movement of the syringe plunger was controlled at a constant rate by a syringe pump (Sage Instruments). The size ($d = 0.3$ to 2.5 mm) of each drop released was controlled by adjusting the timer and syringe pump settings.

The data-logging device was a PC30D analog I/O board (Boston Technology) linked to an IBM compatible computer. It had dual channel direct memory access with a throughput of 200 KHz. Data acquisition was performed using the supplied software package, Waveview, and the sampling frequency was set at 180 Hz.

Materials

The Newtonian fluids consisted of *n*-decane ($> 99\%$ pure, Sigma-Aldrich) and Hyvis 3 polybutene fluid (BP Chemicals) mixed in various proportions to give a viscosity range of 2×10^{-3} to 0.70 Pa·s. Small quantities of PIB (Exxon Vistanex 140-MML polyisobutylene, MW = 2,100,000) were added to some of the Newtonian fluids to make them elastic. The steady shear viscosities of these elastic fluids showed no more than 10% variation over a shear rate range of 1 to 100 s^{-1}. The approximate compositions of the fluids, made on a weight basis, are given in Table 1. Water distilled in an all glass apparatus ($\kappa < 10^{-4} S \cdot m^{-1}$) was used as the aqueous phase.

Procedures

The organic phase was purified and filtered before use by trickling the mixed fluid through a glass column containing granular activated carbon and two glass frits (pore-size range ≈ 16–40 μm). Once sufficient fluid had drained through the column, the fluid was gently mixed on rollers for at least eight hours to ensure it was homogeneous, and then left for at least an hour to allow any entrained air bubbles to be released. The column was regularly cleaned and refilled with fresh activated carbon.

Table 1. Approximate Compositions of Organic Phases (wt. %) and Their Physical Properties at 20 ± 1°C

Fluid	% Hyvis 3	% *n*-decane	% PIB	μ (mP·as)	ρ (kg·m^{-3})	γ (mN·m^{-1})
A	20	80	—	2.20	757	44
B	32	68	—	3.72	773	46
C	53	47	—	11.7	802	30
D	60	40	—	19.8	818	25
E	70	30	—	38.6	825	28
F	70	30	—	42.4	825	34
G	73	27	—	71.4	834	31
H	77	23	—	124	840	29
I	85	15	—	376	854	30
J	88	12	—	699	858	48
K	20	80	0.05	2.58	762	31
L	73	27	0.05	107	840	27
M	85	15	0.05	397	852	31
N1	82	18	—	294	851	31
N2	82	18	—	290	850	46
O1	82	18	0.05	295	851	42
O2	82	18	0.10	295	849	44
O3	82	18	0.15	300	847	42
O4	82	18	0.25	305	852	47

All surfaces that came in contact with the experimental fluids were cleaned thoroughly before use. Glass and teflon materials were washed in detergent, rinsed with water, and then soaked in a freshly made solution of concentrated sodium hydroxide for about an hour. They were then thoroughly rinsed with distilled water and dried in an oven. They syringe tip was thoroughly rinsed and flushed with distilled water.

Experiments for very small drops ($d < 2$ mm), performed using fluids N2 and O1–O4, could not be performed in the manner described above because the drops were too small to break the laser beams and, thus, no readings could be obtained. Therefore, for all of the experiments using these fluids ($d = 0.3$ to 2.5 mm), measurements were made in a 100 mL beaker with a Teflon lid. Drops were released in the same manner as described above, and the coalescence times were measured by stopwatch. In this case, measurement of the coalescence time of discrete drops would lead to large errors, due to the low coalescence time and drop volume, so the time for a batch of twenty drops to coalesce was measured. The drops were released at one-second intervals to minimize the time delay between the release of the first and last drops. The coalescence time was defined as the time for 90% of the drops to coalesce, as it was not possible to determine the time for 50% of the drops to coalesce accurately. Cockbain and McRoberts (1953) measured the coalescence time of groups of drops at an interface and found little difference in the median time obtained from that for single drops, which was attributed to the drops coalescing with the interface in preference to each other. In these experiments the majority of drops coalesced with the interface, although a portion always coalesced with each other, leading to larger drops and differences in the coalescence time. No difference was observed in drop/drop coalescence behavior among the different fluids, so any errors caused by this behavior were assumed to be constant. At least ten measurements of the coalescence time were made for each fluid at each drop size and the results averaged. These experiments were designed to determine whether elastic effects are dependent on drop size; therefore, the coalescence times are only meaningful for comparison with each other.

Interfacial tensions were measured using the digital imaging of pendent drop profiles technique (Lyford, 1996). The results from at least three drops were averaged to determine the interfacial tension. Steady shear viscosity was measured using a Carri-med CSL100 constant stress rheometer, used in the steady rotational mode with a cone and plate geometry. Measurements were made over a range of at least two orders of magnitude in shear rate. Extensional viscosity measurements were determined using a Rheometrics RFX opposing jet apparatus with the 5, 3, 2, 1, and 0.5 mm diameter nozzles. This apparatus was selected, because it allows measurement of elasticity in low viscosity fluids. Despite the acknowledged difficulties with the measurement of a ''true extensional viscosity'' (Hermansky and Boger, 1995), comparisons of data obtained for different fluids as a function of shear rate provides valuable insight into flow behavior under high shear rates where extensional flows can be at least as significant as shear flows. The experimental method is described in detail elsewhere (Hermansky and Boger, 1995). Rheological results are given in Table 1 and Figure 2. All measurements were made at 20 ± 1°C.

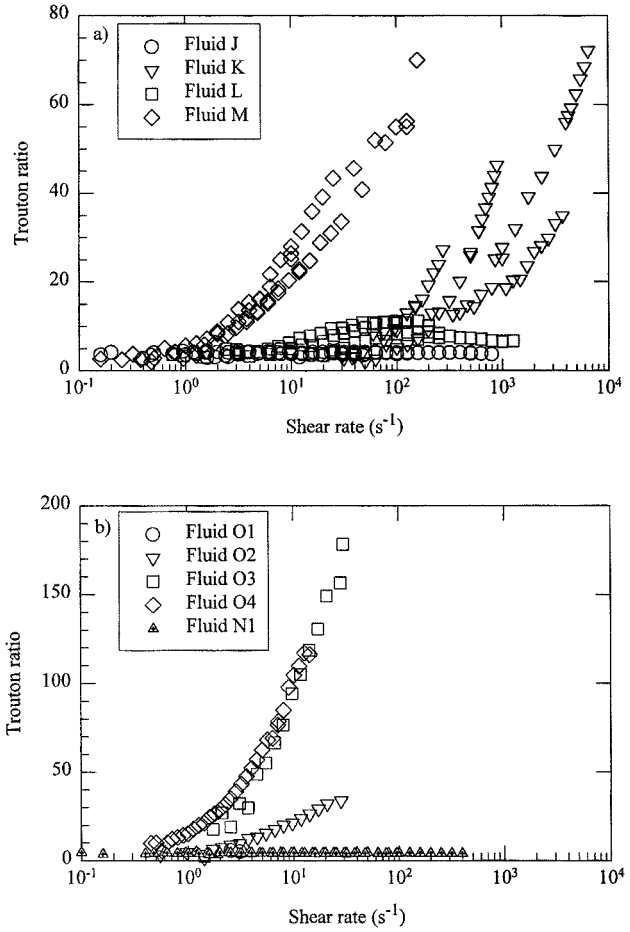

Figure 2. Trouton ratio for fluids (a) J–M, and (b) N1 & O1–O4.

Results

Analysis of drop rest time data

As expected, a spread of drop rest times was obtained for all systems. For the experiments using fluids A–M in the primary apparatus, reproducible coalescence times could be obtained with upwards of twenty measurements, although, where possible, a much greater number of drops were measured. As the overall drop stability increased, less data points were obtained and the spread of data increased. The median coalescence time was used to describe the data, as this has been found to be an accurate measure of the coalescence time (Nielsen et al., 1958). The drop rest time data was found to be more accurately described by a log-normal distribution rather than the more commonly assumed Gaussian distribution, especially for large coalescence times. The drop half-life $\tau_{1/2}$ and geometric standard deviation σ_g for each system were obtained from log-normal distribution plots, as shown in Figure 3, and the results are given in Table 2. Details of the analysis have been described by Davis and Smith (1973).

Median coalescence time

The properties of the organic continuous phase fluids are given in Table 1. Figure 4 indicates that the median drop

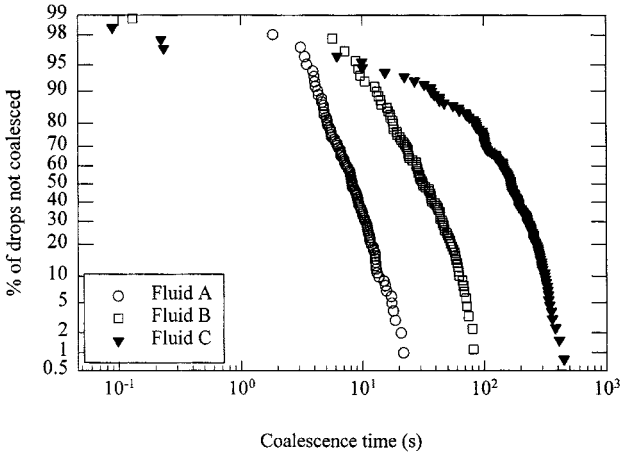

Figure 3. Sample drop rest time data plots based on the log normal distribution function.

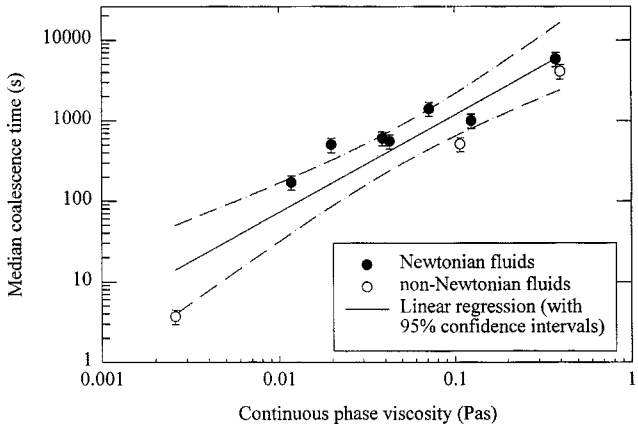

Figure 4. Median coalescence time vs. continuous-phase viscosity for fluids with interfacial tension approximately 29 mN·m^{-1} and drops of diameter approximately 2.5 mm.

coalescence time increased monotonically with the continuous phase viscosity for the fluid systems with interfacial tensions of approximately 29 mN·m^{-1}. The addition of high molecular weight PIB to the continuous phase had little effect, within experimental error, on the coalescence time of the drops with a diameter of approximately 2.5 mm. It was also evident that interfacial tension had a significant effect on coalescence time, and, as the interfacial tension increased, because of greater purity, the coalescence time decreased (see Tables 1 and 2).

Coalescence time results for the experiments conducted with the Newtonian fluid N2 for drops of diameter 0.3–2.5 mm are shown in Figure 5, along with the predictions of two simple coalescence time models. The results are only meaningful for comparison within the group, due to the different experimental technique used. The coalescence time depended linearly upon the drop diameter within the experimental error. Thus, the model of Hartland (1969) was able to successfuly fit the data n_i, α, h_i, and h_c were taken as adjustable parameters incorporated into the proportionality constant for this model; thus, their values could not be determined individually from this data. Gillespie and Rideal's (1956) model, by contrast, does not allow for interfacial mobility, and the best fit to the data, obtained by adjusting the values of h_i and h_c, did not match the observed dependence on drop diameter.

Figure 6 shows the average coalescence time results for the non-Newtonian fluids O1–O4 as a function of the drop diameter, plotted as the ratio of the non-Newtonian to the Newtonian (N2) fluid result vs. drop diameter. The 95% confidence limits for these data were within $\pm$10% of the mean. These non-Newtonian fluids were very similar in all of their physical properties to the Newtonian fluid N2, except in their degree of elasticity, as they contained varying amounts of high molecular weight PIB. Thus, the differences in coalescence behavior observed at very small drop sizes can be attributed to the elasticity of the continuous phase.

Table 2. Drop Stability Results for Fluids

Fluid	d (mm)	u (mm·s^{-1})	N	$\tau_{1/2}$ (s)	Avg. σ_g
A	2.36	92.98	101	8.1	1.52
B	2.20	66.23	89	32	1.96
C	2.38	31.65	129	170	1.99
D	2.96	19.46	47	500	2.45
E	2.40	11.87	47	600	2.92
F	2.36	11.44	45	550	2.99
G	2.50	7.431	28	1,400	2.63
H	2.38	2.600	18	1,000	4.43
I	3.22	1.130	16	5,800	1.95
J	2.48	0.352	35	1,100	3.65
K	2.54	88.91	200	3.7	1.83
L	2.38	4.310	73	510	2.24
M	2.68	1.170	28	4,100	2.46

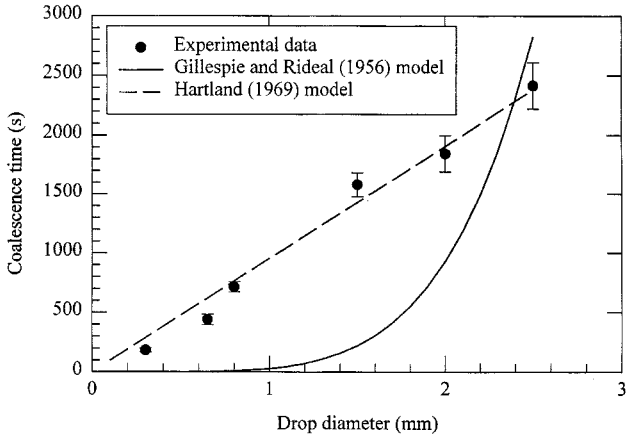

Figure 5. Comparison of experimental results and model predictions for a Newtonian fluid (N2) over a range of drop diameters.

Coalescence time data are the average of 10 experiments each with 95% confidence intervals indicated by the error bars.

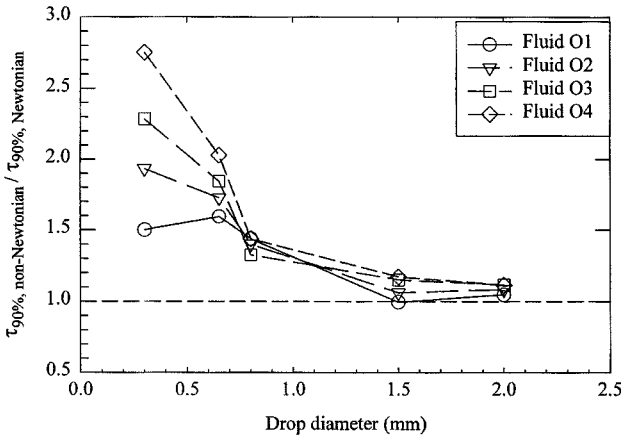

Figure 6. Influence of continuous-phase elasticity on mean coalescence times for 90% of 20 drops for non-Newtonian (O1–O4) fluids in comparison to a Newtonian fluid (N2) of the same steady shear viscosity.

Discussion

For the Newtonian fluid (N2), the coalescence time was found to depend linearly on the diameter of the coalescing drops, fitting the model of Hartland (1969). As expected, the simple hydrodynamic approach of Gillespie and Rideal (1956), was not able to adequately predict the relationship as it does not allow for interfacial mobility or nonuniform film thickness.

For the 2.5 mm drops in fluids with interfacial tensions of approximately 29 $mN \cdot m^{-1}$, the addition of high molecular weight polymer had little effect, within experimental error, on the drop coalescence time (Figure 4). This is in agreement with Williams and Tanner (1970), but is in contrast to many experimental and theoretical results (Tanner, 1965; Metzner, 1971; Kramer, 1974; Leider, 1974; Leider and Bird, 1974; Brindley et al., 1976).

The models of Leider and Bird (1974) and McClelland and Finlayson (1983) both reduce to the Scott equation for the case of zero relaxation time, that is, for an inelastic fluid. Leider and Bird's model (Eq. 3) predicts that the drainage time increases as the fluid's relaxation time increases, with the upper bound of the solution for a constant viscosity fluid given by

$$t = \frac{9\pi\mu_c h_i R^5}{64F}\left(\frac{1}{h_c^2} - \frac{1}{h_i^2}\right)^2 \tag{5}$$

In Leider and Bird's model, the term $\exp(-t/c_2 n\lambda)$ is approximately equal to 0 for $t/\lambda > 0.01$, as c_2 and n are equal to one for this case. Thus, if the relaxation time is of the order of 15 ms, as it was for fluid M, then for any time greater than 1.5×10^{-3}s, Eq. 3 reduces to the Scott equation. Therefore, for these fluids, elasticity has an effect only at the onset of film squeezing, which is in agreement with Metzner's (1971) findings. McClelland and Finlayson's model does not reduce to an explicit solution for highly elastic fluids, although the model does predict that the force required to squeeze out an elastic film will be higher than that for a Newtonian fluid. To obtain the solution for this force, a nonlinear differential equation must be solved for each different fluid.

The drag coefficient vs. Reynolds number curve, given in Figure 7, indicates that during their descent, the 2.5 mm drops behaved as solid spheres. The slight deviations were due to inaccuracies in drop-size measurement, and drop oblateness. The majority of the data is in the creeping flow region and, therefore, inertial effects may be ignored for modeling purposes. A correction for wall effects was deemed unnecessary as the drop diameter divided by the column diameter was always less than 0.1 and, therefore, retardation caused by the proximity of the walls was negligible (Strom and Kintner, 1958). In creeping flow, the maximum shear rate on the surface of a sphere is given by $3u_\infty/2a$. Thus, for fluids K, L, and M, the shear rates on the surface of the falling drops were 105, 5.4 and 1.3 s^{-1} respectively. As all the fluids used in this study had constant steady shear viscosities, the Trouton ratio (Figure 2) can be used to characterize their elasticity as a function of shear rate. Thus, at the calculated shear rates on the surface of the falling drops, the effect of elasticity was small. Also, in creeping flow, the influence of elasticity is insignificant, due to the absence of inertial forces with which elastic forces could interfere. Therefore, the addition of high molecular weight polymer had no effect on the velocity of the falling drops for low Reynolds numbers, and, at higher Reynolds numbers, the elasticity of the fluid was still low and, therefore, also had little effect.

The velocity of the fluid squeezed out between the drop and the interface will depend on the mobility of both interfaces. Lee and Hodgson (1968) developed Eq. 6 for the case of immobile interfaces, and Eq. 7, when allowing for slip at the interfaces, assuming the interfaces are plane parallel (r and z are the radial and axial positions in cylindrical coordinates)

$$u_r = \frac{2Fr}{\pi\mu_c R^4}\left[\left(\frac{h}{2}\right)^2 - z^2\right] \tag{6}$$

$$u_r = u_s + \frac{\partial\gamma/\partial r}{\mu_c h}\left[\left(\frac{h}{2}\right)^2 - z^2\right] \tag{7}$$

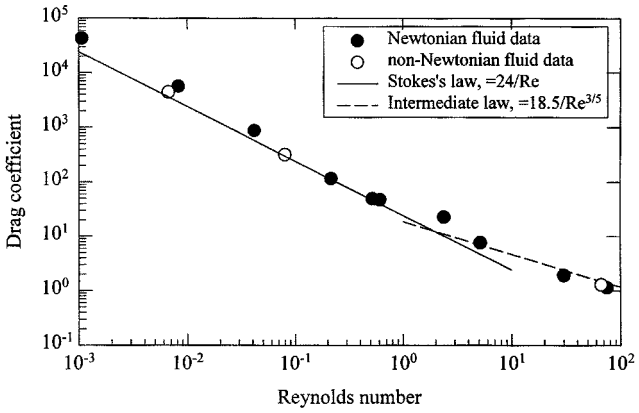

Figure 7. Drag coefficient vs. Reynolds number curve for 2.5 mm drops falling in fluids A–M.

Using Eq. 6 to estimate the velocity of the fluid in the film if the interfaces are immobile with $r = R$ at $z = 0$ and $h = 10^{-6}$m, the maximum velocity for 2.5 mm drops was given by $u = 8\times10^{-8}/\mu_c$. For the viscosity range investigated, this corresponded to Reynolds numbers in the draining film of 10^{-5} to 10^{-11}. If the interfaces are mobile, the velocity of the fluid in the film will be higher than that estimated for immobile interfaces. The velocity of the interface u_s ($\mathrm{m\cdot s^{-1}}$) was calculated as 2×10^{-3} $\mathrm{m\cdot s^{-1}}$ using Eq. 8 (Jeelani and Hartland, 1994), where the interfacial tension gradient was calculated to be -0.33 $\mathrm{N\cdot m^{-2}}$ from experimental data using Eq. 9 (Hartland and Jeelani, 1994). Although Eq. 9 assumes immobile interfaces, it is the only method available to calculate $\partial\gamma/\partial r$, and was, therefore, used as an approximation. Substituting this value into Eq. 7, the second term was found to be much smaller than the surface velocity and, therefore, the radial velocity was initially approximately equivalent to the surface velocity

$$u_s = \left(\frac{Fah_i}{\pi\mu_d R^3}\right)\left[1+\left(\frac{\pi R^3}{2Fh_i}\right)\left(\frac{\partial\gamma}{\partial r}\right)_{Ri}\right] \tag{8}$$

$$\left(\frac{\partial\gamma}{\partial r}\right)_{Ri} = -\frac{2Fh_i}{\pi R^3} \tag{9}$$

The calculated surface velocity corresponded to Reynolds numbers of 2×10^{-6} to 8×10^{-4} for the viscosity range investigated. When the interfaces are fully mobile, the interfacial tension gradient is zero and, therefore, from Eqs. 6 and 7, the velocity of the film was estimated to be 0.2 $\mathrm{m\cdot s^{-1}}$, which corresponds to Reynolds numbers in the range of 2×10^{-4} to 8×10^{-2}. The above calculations indicate that flow of the squeezed film for 2.5 mm drops was laminar and, in the creeping flow region, even when the interface was fully mobile. Therefore, due to the absence of inertia in the squeezing film, elastic effects are expected to be small for drops of this size.

For Newtonian fluids, the shear stress at the interface is equal to the viscosity of the fluid multiplied by the velocity gradient. This relation also holds for the viscoelastic fluids used in this study, because their viscosities were independent of shear rate, as is the case for Newtonian fluids. If the interfaces are assumed immobile, Eq. 6 may be used to calculate the velocity gradient, which leads to Eq. 10 (Jeelani and Hartland, 1994; Lee and Hodgson, 1968). Equation 11 is obtained upon substitution for R (Derjaguin and Kussakov, 1939)

$$\tau_r' = -\frac{2Fh}{\pi R^4}r \tag{10}$$

$$\tau_R' = -\left(\frac{8}{3a^3(\Delta\rho g)^{1/2}}\right)\left(\frac{3\gamma}{2}\right)^{3/2}h \tag{11}$$

From Eq. 11, the maximum shear stress at the interface for a 2.5 mm diameter drop was -0.33 $\mathrm{N\cdot m^{-2}}$, occurring at the film periphery. This corresponded to shear rates of 129, 3.1, and 0.8 $\mathrm{s^{-1}}$ for the fluids K, L, and M, respectively. At these low shear rates, the corresponding Trouton ratio for each non-Newtonian fluid was approximately that of a Newtonian fluid, so elastic effects were small. When the interfaces are mobile, the velocity gradient will decrease and, therefore, the shear stress, and the corresponding shear rate, will also decrease. This will decrease the effect of elasticity. As the interfaces were likely to have a significant degree of mobility, elasticity is not expected to have had a significant effect on the coalescence time for 2.5 mm drops in these fluids, and this was confirmed by the experimental results in Figure 4.

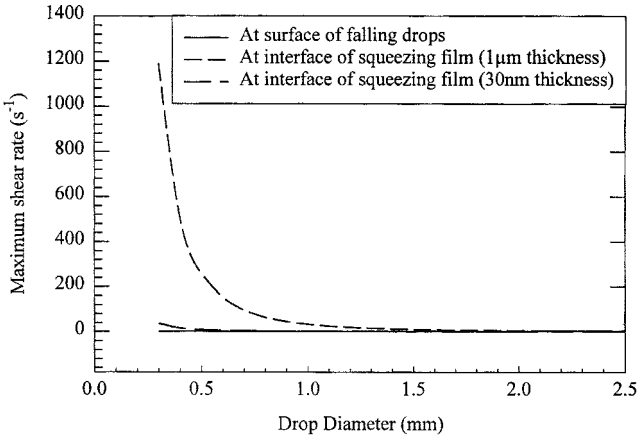

Figure 8. Maximum shear rates at the surface of the falling drops, and at the interface of the squeezing film.

Rates calculated using Stokes law and Eq. 11, respectively.

The terminal velocities of the smaller drops could not be measured, so they were estimated using Stokes' law. Figure 7 indicates that Stokes law was followed for large drops falling in fluids with a similar viscosity to fluids N2 and O1–O4, so for smaller drops, the assumption of creeping flow was appropriate. Using this method, the terminal velocity of drops with a diameter of approximately 0.3 mm, for example, was calculated to be 0.025 $\mathrm{mm\cdot s^{-1}}$. The maximum shear rate at the surface of the falling drops was thus estimated to be less than 2 $\mathrm{s^{-1}}$ for drops of less than 2.5 mm diameter (see Figure 8). At such low shear rates, the influence of elasticity on the falling drops was expected to be negligible, based on the Trouton ratio, except for the more elastic fluids studied (O3 and O4), where a small effect was expected.

For squeezing film flow, Eq. 11 indicates that the shear stress at the interface is inversely proportional to the drop radius cubed. Therefore, as the drop size decreases, the shear stress and shear rate increase significantly, as shown in Figure 8, assuming immobile interfaces. The experiments conducted with drops of different diameters confirmed that elastic effects on coalescence are dependent on drop size (Figure 6). For very small drops, elasticity in the continuous phase significantly increased the coalescence time, whereas no significant effect was detected for drops of 1.5 mm diameter or larger. This cannot be simply explained by the stress overshoot mechanism proposed by Phan-Thien et al. (1987), although the estimated Weissenberg numbers (approximately 0.8–50 for fluid O4) are greater than the cutoff they determined for viscoelastic effects in constant-speed squeezing. The overshoot mechanism implies that viscoelastic effects in-

crease as the fluid elasticity increases, as we observed, but also that they increase as the initial squeezing velocity increases. The initial velocity in these coalescence experiments is expected to be related to the terminal approach velocity of the drop falling towards the interface, which decreases with decreasing drop size, whereas the effects of elasticity were observed to *increase* as drop size decreased.

It is proposed that the observed dependence of elastic effects on drop size occurred because the shear rate at the interface of the smaller drops was high enough for the non-Newtonian fluids to exhibit some elastic characteristics. As shown in Figure 8, the maximum shear rate at the interface of the squeezing film increases rapidly with decreasing drop size and with increasing film thickness. Sample curves are shown for squeezing film thicknesses of 1 μm and 30 nm, chosen to be representative of the initial and final film thicknesses during the coalescence process respectively (Murdoch and Leng, 1971; Liem and Woods, 1974). For a film thickness of around 1 μm, the maximum shear rates at the interface are expected to be relatively large for drops of less than about 1 mm. This would result in the Trouton ratio for the non-Newtonian fluids (O1−O4) being much larger than that for the Newtonian fluid (N2) when the film began to thin, and so elastic effects would be significant. It must be noted, however, that the interfaces are not immobile, as assumed in Eq. 11, and that the shear rate will decrease as the film thins. Furthermore, Eq. 11 is only valid if the interfaces are plane parallel and so, only applies after the drop has deformed when it is very close to the interface. Therefore, the elastic effects were probably less than predicted by the upper curve in Figure 8, but for the smaller drops it was still expected that the non-Newtonian fluids would exhibit elastic effects for a significant part of the coalescence process. It may be inferred that elastic effects are most significant when the drop just reaches the interface, before notable thinning has occurred.

For two fluids, one Newtonian and the other non-Newtonian of the same shear viscosity, the effective viscosity in squeezing, or elongational flow, is greater for the non-Newtonian fluid, providing the shear rate is high enough. The greater effective viscosity reduces the rate at which the film thins, thereby increasing the coalescence time. This result is significant in relation to the stability of emulsions formed with non-Newtonian fluids. It is apparent that elastic effects are dependent on shear rate, which varies with drop size. For elasticity to affect coalescence rates, the drop size must be small enough that the fluid will exhibit elastic characteristics at the interfacial shear rate. Therefore, in considering the effect of large polymers on emulsion stability, the fluid elasticity should be determined to enable prediction of the shear rate at which elastic effects become significant. Combining this with knowledge of the fluid's physical properties, and using Eq. 11, the critical drop size at which elasticity will affect emulsion stability may be determined. It should be noted that the calculations for shear rate and drop size assume immobile interfaces, so the results will be an overestimation of the values required. Allowance for this should be made when designing an emulsion system. For drops larger than the critical size, elasticity will be insignificant and the stability of Newtonian and non-Newtonian emulsions of the same continuous phase viscosity will be the same. Below the critical drop size, the non-Newtonian emulsion will be significantly more stable than the Newtonian case. For the fluids used in this study, the critical drop diameter calculated such that elastic effects are significant even when the film thins to 30 nm, and assuming immobile interfaces, was estimated to be in the range 0.8−1.1 mm. This corresponds with the experimental results shown in Figure 6, which show the coalescence time for the non-Newtonian fluids increasing relative to that for the Newtonian fluid at drop diameters of 0.8 mm and lower. It is not unreasonable to expect this drop size in an emulsion (Lorbach and Hatton, 1988; Stevens et al., 1996) and so, with careful formulation, enhanced stability may be obtained, using elastic non-Newtonian fluids.

The above finding will have a significant effect on the formulation of many emulsion systems. For example, with emulsion liquid membranes, increased stability may be achieved by the addition of a suitable high molecular weight polymer, rather than increasing the bulk viscosity which would decrease mass transfer, or by adding surfactants which can also have adverse effects on mass transfer (Mikucki and Osseo-Asare, 1986). It has been shown that for an emulsion liquid membrane, greater chromium extraction may be achieved using a viscoelastic membrane, rather than a purely Newtonian one, which was attributed to greater stability of the viscoelastic membrane (Stevens et al., 1996). The increase in effective viscosity, caused by polymer addition, does not decrease mass transfer if the polymer is only present at dilute concentrations, because the rate of diffusion is largely dependent on the solvent viscosity (Metzner, 1971; Ponter and Davies, 1966). If a too high a polymer concentration is used, however, diffusion rates may be affected, and dispersion of the internal phase may be hindered (Stevens et al., 1996).

Conclusion

The effect of continuous phase viscosity and elasticity on drop coalescence time at a planar interface was investigated. It was found that the effects of elasticity in the continuous phase caused significant increases the coalescence times for drops of less than 1 mm diameter in the systems studied. As predicted from the estimated interfacial shear rates and the measured Trouton ratio of the fluids tested, elasticity becomes significant in the coalescence process as the drop size decreases.

The results indicated that emulsion stability may be increased by the addition of a suitable polymer to the continuous phase. The extent of stabilization was dependent on the rheological properties of the polymer solution, and the dispersed-phase drop size. A method has been proposed which enables an estimation of the conditions at which elastic effects become significant. This relies on knowledge of the physical and rheological properties of the continuous and dispersed phases, in particular, the Trouton ratio of the continuous phase.

Acknowledgments

This work was funded by City West Water Ltd., the Advanced Mineral Products Special Research Centre, and the Australian Research Council. The polybutene fluids were supplied by BP Chemicals Ltd.

Notation

a = drop radius, m
C_D = drag coefficient, $4\Delta\rho dg/3\rho_c u^2$
d = drop diameter, m
F = force, N
g = acceleration due to gravity, $m \cdot s^2$
h = film thickness, m
h_c = film thickness at drop rupture, m
h_i = film thickness when drop initially rests at interface, m
m, m' = power law parameters, $N \cdot m^{-2} \cdot s^{-n,n'}$
M_g = geometric mean, s
n, n' = power law slopes
N = number of drops
N_1 = primary normal stress difference, $N \cdot m^{-2}$
R = radius of barrier ring, m
Re = Reynolds number, $\rho_c ud/\mu_c$
t = time, s
Tr = Trouton ratio
u = velocity, $m \cdot s^{-1}$
u_i = initial velocity of top plate in squeezing flow between two plates, $m \cdot s^{-1}$
u_r = radial velocity, $m \cdot s^{-1}$
u_∞ = terminal velocity, $m \cdot s^{-1}$
Wi = Weissenberg number
α = angle of the edge of the film to the vertical axis
γ = interfacial tension, $N \cdot m^{-1}$
$\dot{\gamma}$ = shear rate, s^{-1}
κ = conductivity, $S \cdot m^{-1}$
λ = relaxation time, s
μ_c = continuous phase viscosity, $Pa \cdot s$
μ_d = dispersed phase viscosity, $Pa \cdot s$
ρ = density, $kg \cdot m^{-3}$
σ_g = geometric standard deviation
τ = shear stress, $N \cdot m^{-2}$
τ_r = shear stress at radius r, $N \cdot m^{-2}$
$\tau_{1/2}$ = time taken for half the drops to coalesce, half life, median coalescence time, s
$\tau_{90\%}$ = time taken for 90% of the drops to coalesce, s

Literature Cited

Barber, A. D., and S. Hartland, "The Effects of Surface Viscosity on the Axisymmetric Drainage of Planar Liquid Films," *Can. J. Chem. Eng.*, **54**, 279 (1976).

Brindley, G., J. M. Davies, and K. Walters, "Elastico-Viscous Squeeze Films. Part I, "*J. Non-Newtonian Fluid Mech.*, **1**, 19 (1976).

Cockbain, E. G., and T. S. McRoberts, "The Stability of Elementary Emulsion Drops and Emulsions," *J. Coll. Sci.*, **8**, 440 (1953).

Davis, S. S., and A. Smith, "The Interpretation of Droplet Coalescence Data using the Log Normal Distribution," *Kolloid-Z.u.Z. Poly.*, **251**, 337 (1973).

Dell'Aversana, P., J. R. Banavar, and J. Koplik, "Suppression of Coalescence by Shear and Temperature Gradients," *Phys. Fluids*, **8**, 15 (1996).

Dell'Aversana, P., V. Tontodonato, and L. Carotenuto, "Suppression of Coalescence and Wetting: The Shape of the Interstitial Film," *Phys. Fluids*, **89**(9), 2475 (1997).

Derjaguin, B. V., and M. Kussakov, *Acta Physicochim. U.S.S.R.*, **10**, 25 (1939).

Gillespie, T., and E. K. Rideal, "The Coalescence of Drops at an Oil-Water Interface," *Trans. Faraday Soc.*, **52**, 173 (1956).

Hartland, S., "The Coalescence of a Liquid Drop at a Liquid-Liquid Interface. Part II: Film Thickness," *Trans. Instn. Chem. Engrs.*, **45**, T102 (1967a).

Hartland, S., "The Coalescence of a Liquid Drop at a Liquid−Liquid Interface. Part III: Film Rupture," *Trans. Instn. Chem. Engrs.*, **45**, T109 (1967b).

Hartland, S., "The Profile of the Draining Film Between a Rigid Sphere and a Deformable Fluid-Liquid Interface," *Chem. Eng. Sci.*, **24**, 987 (1969).

Hartland, S., and S. A. K. Jeelani, "Effect of Interfacial Tension Gradients on Emulsion Stability," *Colloids Surfaces A: Physicochem. Eng. Aspects*, **88**, 289 (1994).

Hermansky, C. G., and D. V. Boger, "Opposing-Jet Viscometry of Fluids with Viscosity Approaching that of Water," *J. Non-Newt. Fluid Mech.*, **56**, 1 (1995).

Jeelani, S. A. K., and S. Hartland, "Effect of Interfacial Mobility on Thin Film Drainage," *J. Coll. Int. Sci.*, **164**, 296 (1994).

Kramer, J. M., "Large Deformations of Viscoelastic Squeeze Films," *Appl. Sci. Res.*, **30**, 1 (1974).

Lang, S. B., and C. R. Wilkie, "A Hydrodynamic Mechanism for the Coalescence of Liquid Drops: I. Theory of Coalescence at a Planar Interface," *Ind. Eng. Chem. Fundam.*, **10**, 329 (1971).

Lee, J. C., and T. D. Hodgson, "Film Flow and Coalescence: I. Basic Relations, Film Shape and Criteria for Interface Mobility," *Chem. Eng. Sci.*, **23**, 1375 (1968).

Leider, P. J., and R. B. Bird, "Squeezing Flow Between Parallel Disks. I. Theoretical Analysis," *Ind. Eng. Chem. Fundam.*, **13**, 336 (1974).

Liem, A. J. S., and D. R. Woods, "Application of the Parallel Disc Model for Uneven Film Thinning," *Can. J. Chem. Eng.*, **52**, 222 (1974).

Lorbach, D., and T. Hatton, "Polydispersity and Backmixing Effects in Diffusion Controlled Mass Transfer with Irreversible Chemical Reaction: an Analysis of Liquid Emulsion Membrane Processes," *Chem. Eng. Sci.*, **43**, 405 (1988).

Lyford, P., "The Influence of the Marangoni Effect on Organic/Aqueous Phase Displacement," PhD Thesis, Univ. of Melbourne, Dept. of Chemical Engineering (1996).

McClelland, M. A., and B. A. Finlayson, "Squeezing Flow of Elastic Liquids," *J. Non-Newt. Fluid Mech.*, **13**, 181 (1983).

Metzner, A. B., "Extensional Primary Field Approximations for Viscoelastic Media," *Rheol. Acta.*, **10**, 434 (1971).

Mikuchi, B., and K. Osseo-Asare, "Metal Extraction with Liquid Surfactant Membranes: The Role of the Emulsifying Agent," *Proc. Int. Sol. Ex. Conf.*, Vol. I, Munich, Germany, 561 (Sept. 11−16, 1986).

Murdoch, P. G., and D. E. Leng, "The Mathematical Formulation of Hydrodynamic Film Thinning and its Application to Colliding Drops Suspended in a Second Liquid: II," *Chem. Eng. Sci.*, **26**, 1881 (1971).

Nielsen, L. E., R. Wall, and G. Adams, "Coalescence of Liquid Drops at Oil-Water Interfaces," *J. Colloid. Sci.*, **13**, 441 (1958).

Phan-Thien, N., F. Sugeng, and R. I. Tanner, "The Squeeze-Film Flow of a Viscoelastic Fluid," *J. Non-Newt. Fluid Mech.*, **24**, 97 (1987).

Ponter, A. B., and G. A. Davies, "Comparison of Diffusion of Carbon Dioxide into Hydrocarbon Systems and Polymeric Solutions," *Nature*, **210**, 837 (1966).

Scott, J. R., "Theory and Application of the Parallel-Plate Plastimeter," *Trans. Inst. Rubber Ind.*, **7**, 169 (1931).

Stefan, J., and K. Sitzgber, "Versuche über die scheinbare adhäsion," *Akad. Wiss. Math. Natur Wien Sitzber.*, **69**, 713 (1874).

Stevens, G. W., C. Chang, and M. E. Mackay, "Stabilizing Emulsion Liquid Membranes," *Sep. Sci. Technol.*, **31**(8), 1025 (1996).

Strom, J. R., and R. C. Kintner, "Wall Effect for the Fall of Single Drops," *AIChE J.*, **4**, 153 (1958).

Tanner, R. I., "Some Illustrative Problems in the Flow of Viscoelastic non-Newtonian Lubricants," *ASLE Trans.*, **8**, 179 (1965).

Vrij, A., and J. T. G. Overbeek, "Rupture of Thin Liquid Films due to Spontaneous Fluctuations in Thickness," *J. Amer. Chem. Soc.*, **90**, 3074 (1968).

Williams, G., and R. I. Tanner, "Effects of Combined Shearing and Stretching in Viscoelastic Lubrication," *J. Lubric. Tech.*, **92**, 216 (1970).

Yiantsios, S. G., and R. H. Davis, "On the Buoyancy-Driven Motion of a Drop towards a Rigid Surface or a Deformable Interface," *J. Fluid Mech.*, **217**, 547 (1990).

Zapryanov, Z., A. K. Malhotra, N. Aderangi, and D. T. Wasan, "Emulsion Stability: An Analysis of the Effects of Bulk and Interfacial Properties on Film Mobility and Drainage Rate," *Int. J. Multiphase Flow*, **9**, 105 (1983).

Manuscript received May 22, 1998, and revision received Mar. 18, 1999.